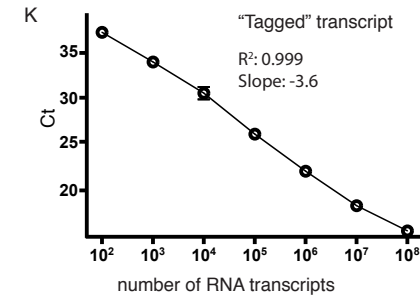
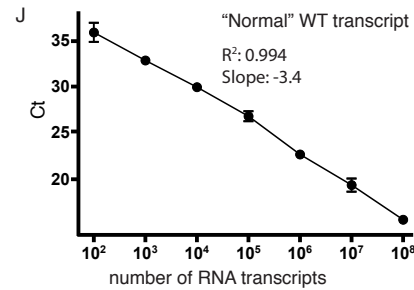
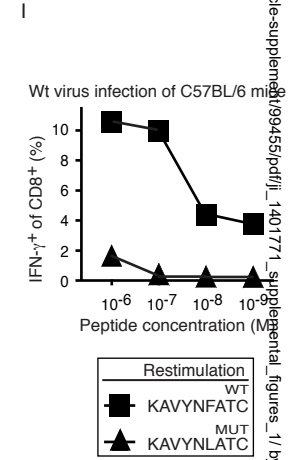
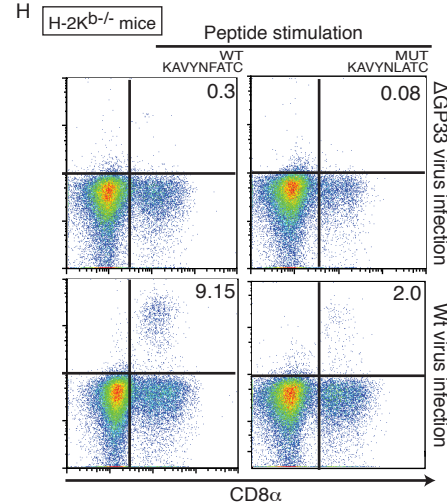
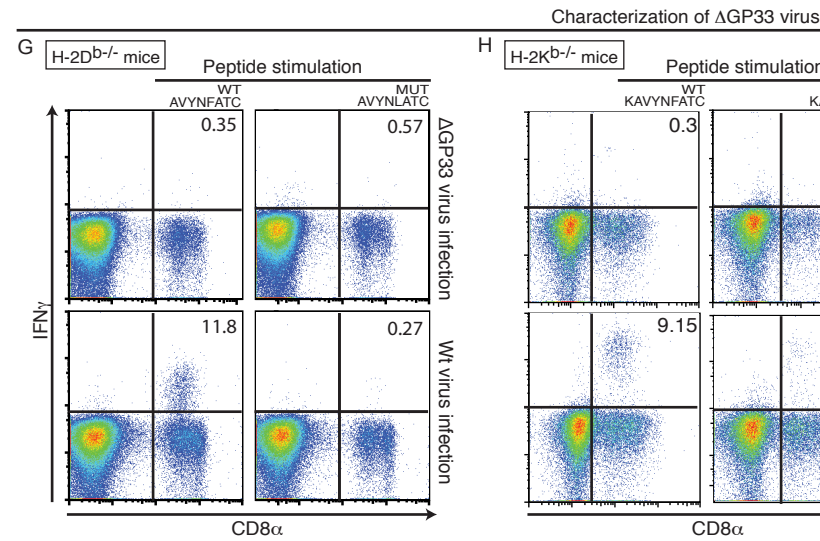
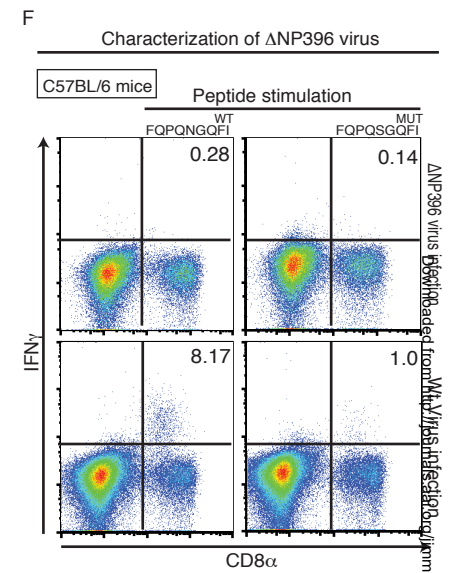
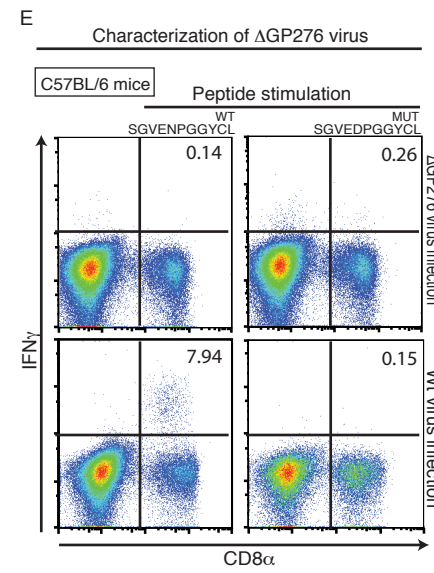
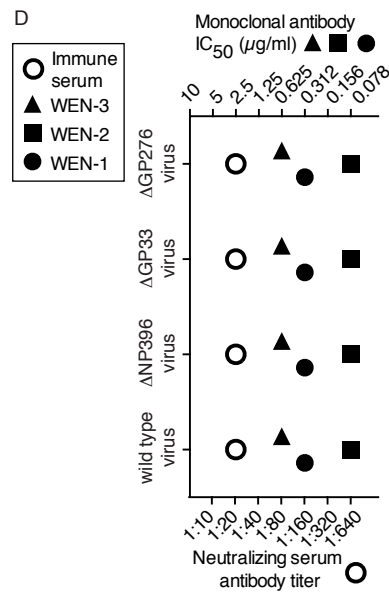
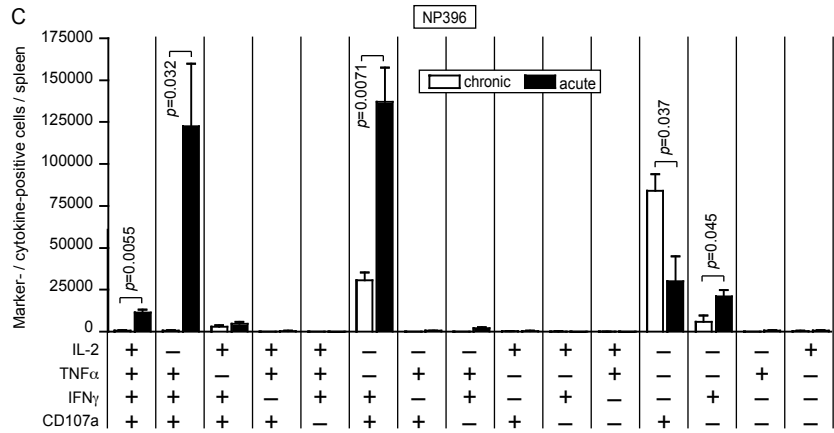
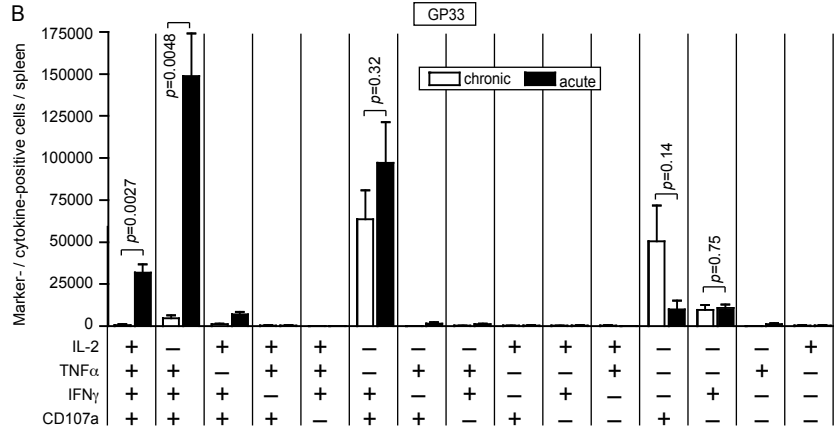
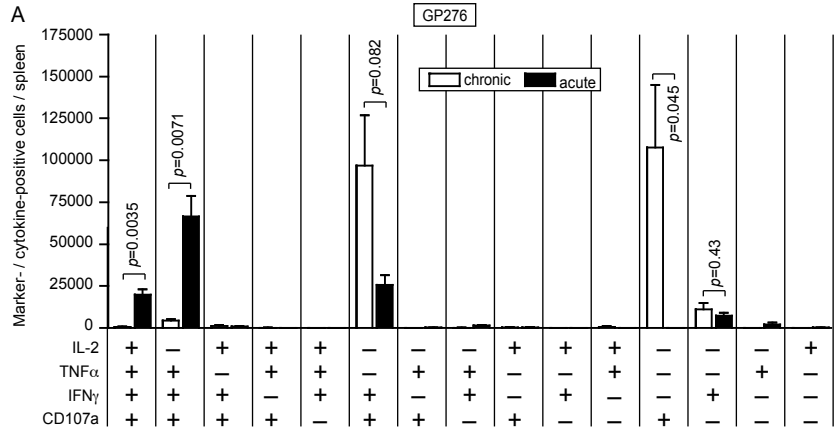


Figure S1



**L**

Transcript (type/copies)	Detection (Ct)	
	Tag	WT
WT 10 <sup>6</sup>	> 45	22
Tag 10 <sup>6</sup>	24	> 45

bioRxiv preprint doi: <https://doi.org/10.1101/140177>; this version posted September 1, 2017. The copyright holder for this preprint (which was not certified by peer review) is the author/funder, who has granted bioRxiv a license to display the preprint in perpetuity. It is made available under aCC-BY-NC-ND 4.0 International license.

## Figure S1. Characterization and validation of experimental model and tools.

**A-C.** To compare T cell functionality in chronic and acute infection we infected C57BL/6 mice with LCMV Armstrong (causing acute self-limiting infection ; « acute ») or LCMV strain Clone 13 (« chronic »). On day 20 we assessed the functionality of GP276- (A), GP33- (B) and NP396-specific (C) CTLs by intracellular cytokine assays. All possible combinations of IL-2, TNF- $\alpha$ , IFN- $\gamma$  and CD107a expression are displayed. The data presented in Fig. 1A represent an extract of this data set. Bars represent the mean $\pm$ SEM of three mice per group.

**D:** We tested the neutralization sensitivity of  $\Delta$ GP276 virus,  $\Delta$ GP33 virus,  $\Delta$ NP396 virus and wild type control virus to three monoclonal neutralizing antibodies (WEN-1, WEN-2, WEN-3) and to a pool of LCMV-convalescent mouse serum.

**E-I:** To characterize genetically engineered CTL epitope-deficient mutant viruses we infected C57BL/6 mice with 200 PFU of the indicated viruses. Twenty days later we performed intracellular IFN- $\gamma$  staining to assess the responsiveness of splenic CD8<sup>+</sup> T cells to the indicated wildtype and mutant epitopes, respectively. E :  $\Delta$ GP276 virus or wildtype (wt) control virus. Wildtype GP276 epitope (SGVENPGGYC) versus mutated (mut) epitope of the  $\Delta$ GP276 virus (SGVEDPGGYC). Representative plots are presented from 2 experiments with 3 mice each. F:  $\Delta$ NP396 virus or wt control virus. Wildtype NP396 epitope (FQPQNGQFI) versus mutated epitope of the  $\Delta$ NP396 virus (FQPQSGQFI). Representative plots are presented from 2 experiments with 3 mice each. G-I: The GP33 epitope can be presented by H-2D<sup>b</sup> as well as by H-2K<sup>b</sup>. The minimal peptide motifs are KAVYNFATC and AVYNFATC, respectively, but the former also binds to H-2K<sup>b</sup>. To individually characterize the mutated GP33 epitope of the  $\Delta$ GP33 virus in the context of either MHC molecule, we infected H-2D<sup>b</sup>- (G) and H-2K<sup>b</sup>-deficient mice (H) with 200 PFU of  $\Delta$ GP33 virus or wt control virus. Intracellular IFN- $\gamma$  staining were performed to assess the responsiveness of splenic CD8<sup>+</sup> T cells to the wildtype GP33 epitope (AVYNFATC and KAVYNFATC for H-2D<sup>b</sup>- and H-2K<sup>b</sup>- mice, respectively) and to the mutated epitope of the  $\Delta$ GP33 virus (AVYNLATC and KAVYNLATC for H-2D<sup>b</sup>- and H-2K<sup>b</sup>- mice, respectively). All of the above experiments were performed with 10<sup>-6</sup> M peptide for restimulation, resulting in residual recognition of the mutated GP33 epitope (KAVYNLATC) by H-2D<sup>b</sup>-restricted CD8<sup>+</sup> T cells of H-2K<sup>b</sup>- mice. Representative plots are presented from triplicate samples of 4 mice per group tested in two independent experiments (G, H). In (I) we performed peptide titration experiments with CD8<sup>+</sup> T cells of wt virus-infected C57BL/6 mice, demonstrating that responsiveness to the mutated peptide KAVYNLATC was lost at more physiological peptide concentrations of 10<sup>-7</sup> M or lower. Representative plots are presented from triplicate analyses of 2 mice per group. All FACS plots are gated on B220<sup>-</sup> lymphocytes.

**J-L:** To determine the accuracy and specificity of our TaqMan RT-PCR assays for the individual quantification of epitope-mutant and wildtype viruses in co-infected mice we generated serial 10-fold dilutions of *in vitro* transcript RNA comprising the TaqMan target sequence in the nucleoprotein ORF of the respective LCMV S segments. *In vitro* transcripts were either of normal viral nucleotide sequence (J; present in epitope-mutant viruses) or of “tagged” viral nucleotide sequence (K; present in wildtype virus utilized for co-infected experiments). We performed TaqMan RT-PCR assays with matching primer and probe sets to record Ct values at which a specific signal was detected. Symbols represent the mean±SD of three replicate reactions per dilution. Based on these results we calculated the slope and R<sup>2</sup> values as indicated. L: The two primer-probe sets, designed to detect either normal viral nucleotide sequence or tagged viral nucleotide sequence were tested on 10<sup>6</sup> copies of matching or mismatched template, respectively, demonstrating the target specificity of both RT-PCR assays.

Figure S2

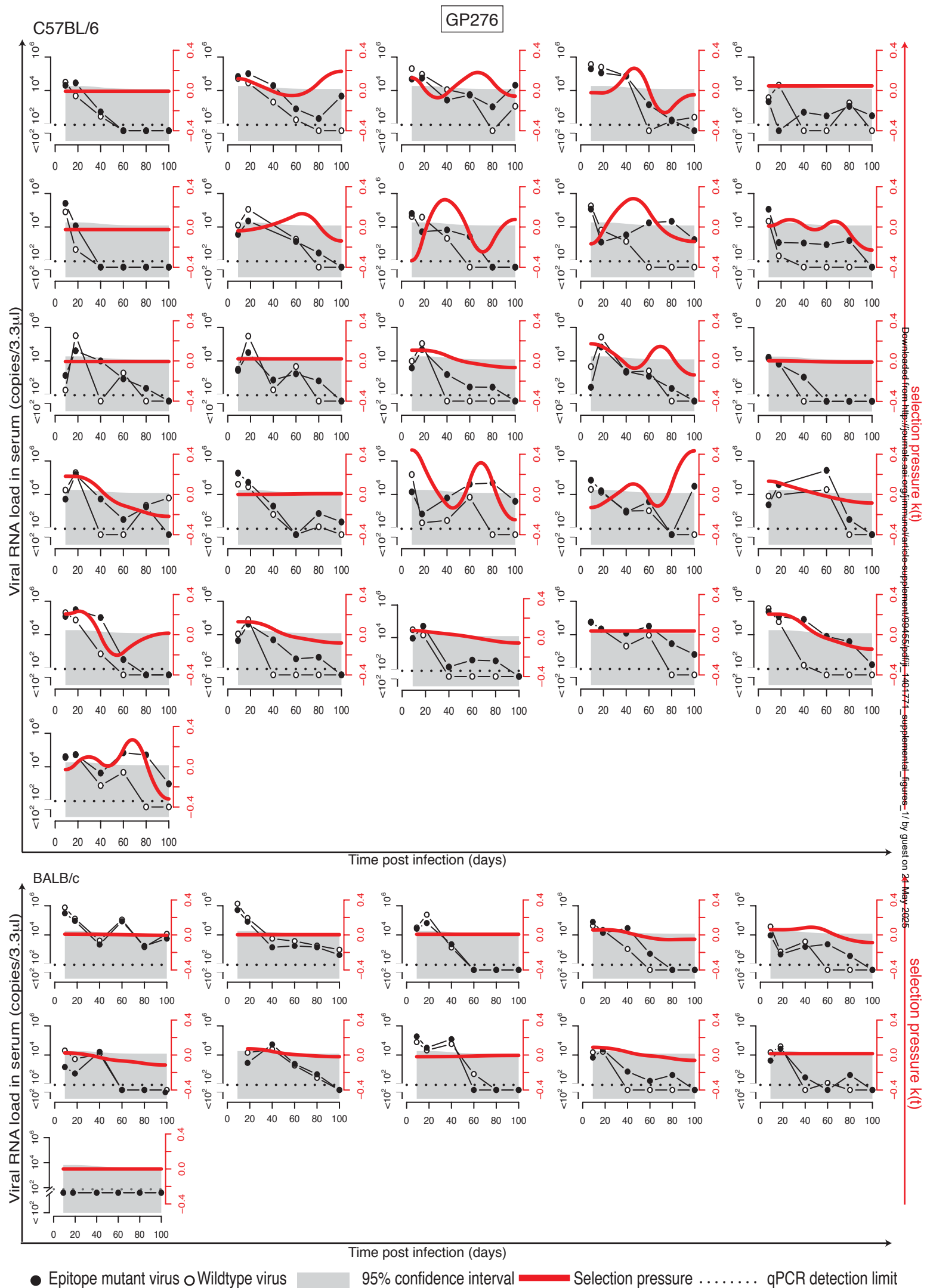
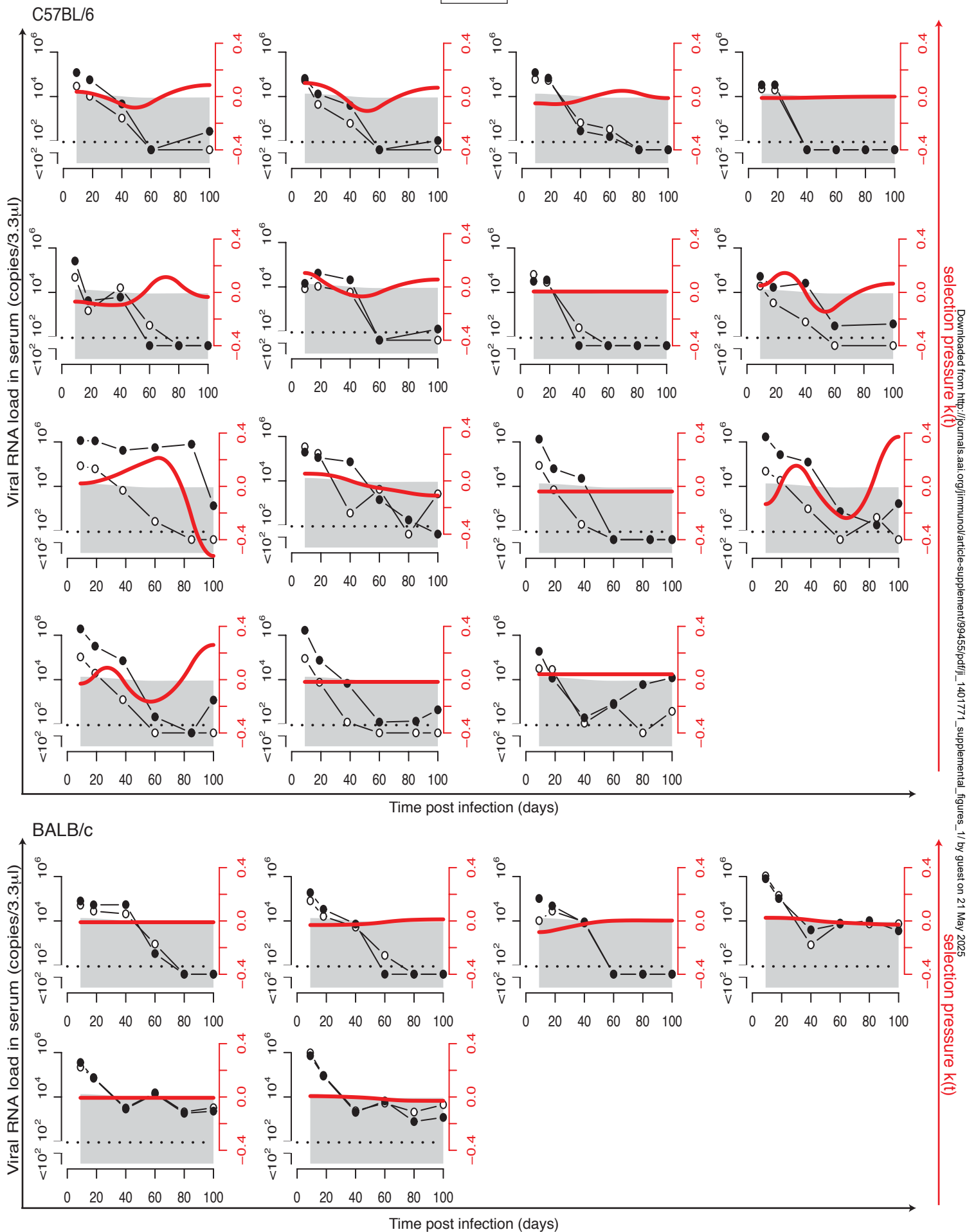


**Figure S2: GP276-specific CTL selection pressure in protracted LCMV infection.**

We infected C57BL/6 (top panels) and BALB/c mice (bottom panels) with  $2 \times 10^5$  PFU of  $\Delta$ GP276 virus in combination with  $2 \times 10^6$  PFU of wildtype LCMV (compare schematic in Fig. 1C). From serum samples collected on day 9, 20, 40, 60, 80 and 100 we quantified each type of virus individually by TaqMan RT-PCR (black circles :  $\Delta$ GP276; empty circles : wildtype virus). Time-dependent selection coefficients  $k(t)$  were calculated as schematically outlined in Figure 1G-I (for details see Materials & Methods) and are shown as red lines. The grey shaded area denotes the 95% confidence interval of background noise in  $k(t)$  in the absence of epitope-specific selection pressure. Each plot shows an individual C57BL/6 or BALB/c mouse from 3 experiments, which were combined for analysis. Select plots from this figure were chosen for display in Figure 2.

Figure S3

GP33



● Epitope mutant virus ○ Wildtype virus █ 95% confidence interval — Selection pressure ..... qPCR detection limit

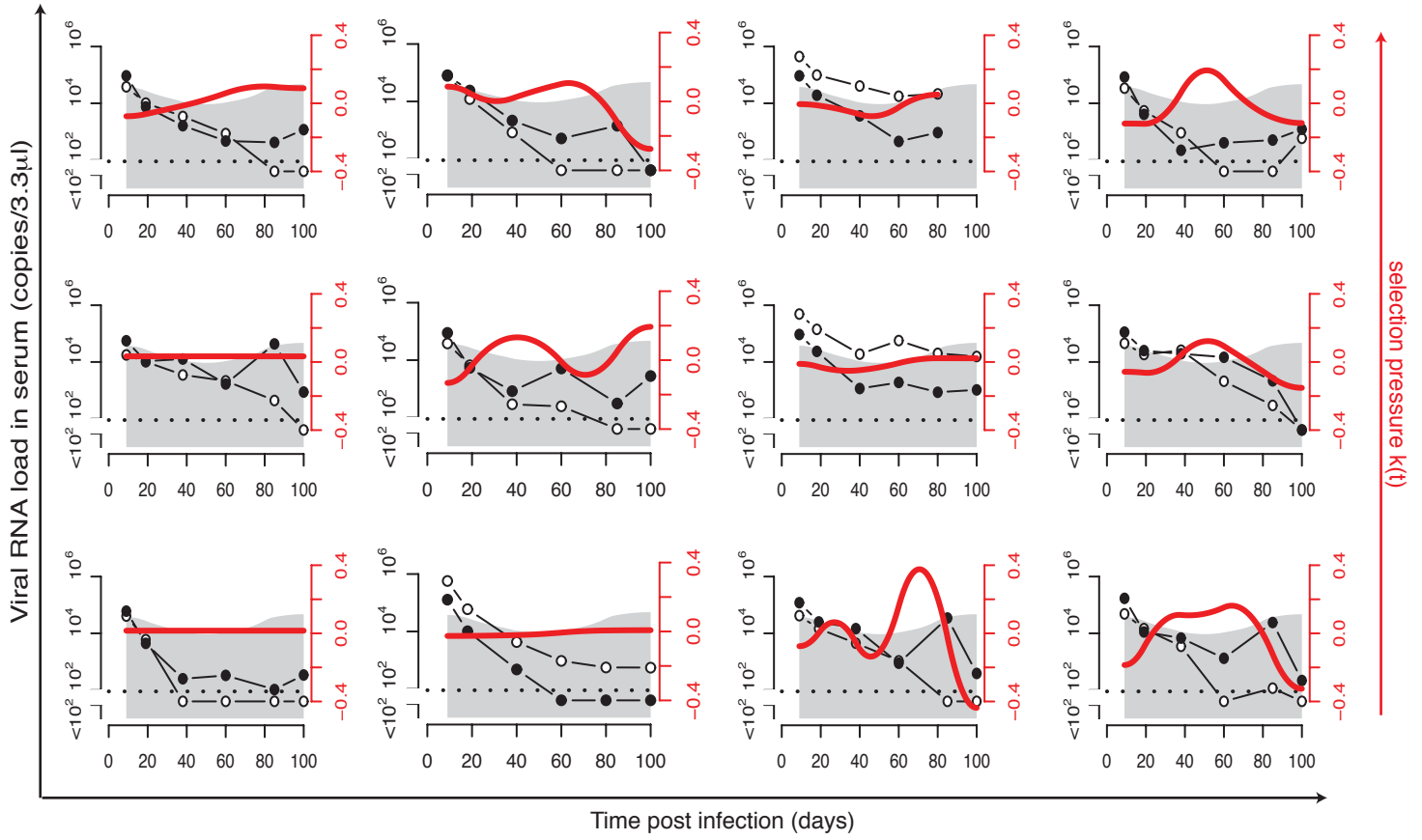
**Figure S3: GP33-specific CTL selection pressure in protracted LCMV infection.**

We infected C57BL/6 (top panels) and BALB/c mice (bottom panels) with  $2 \times 10^5$  PFU of  $\Delta$ GP33 virus in combination with  $2 \times 10^6$  PFU of wildtype LCMV (compare schematic in Fig. 1C). From serum samples collected on day 9, 20, 40, 60, 80 and 100 we quantified each virus individually by TaqMan RT-PCR (black circles :  $\Delta$ GP33; empty circles : wildtype virus). Time-dependent selection coefficients  $k(t)$  were calculated as schematically outlined in Figure 1G-I (for details see Materials & Methods) and are shown as red lines. The grey shaded area denotes the 95% confidence interval of background noise in  $k(t)$  in the absence of epitope-specific selection pressure. Each plot shows an individual C57BL/6 or BALB/c mouse from 3 experiments, which were combined for analysis. Select plots from this figure were chosen for display in Figure 2.

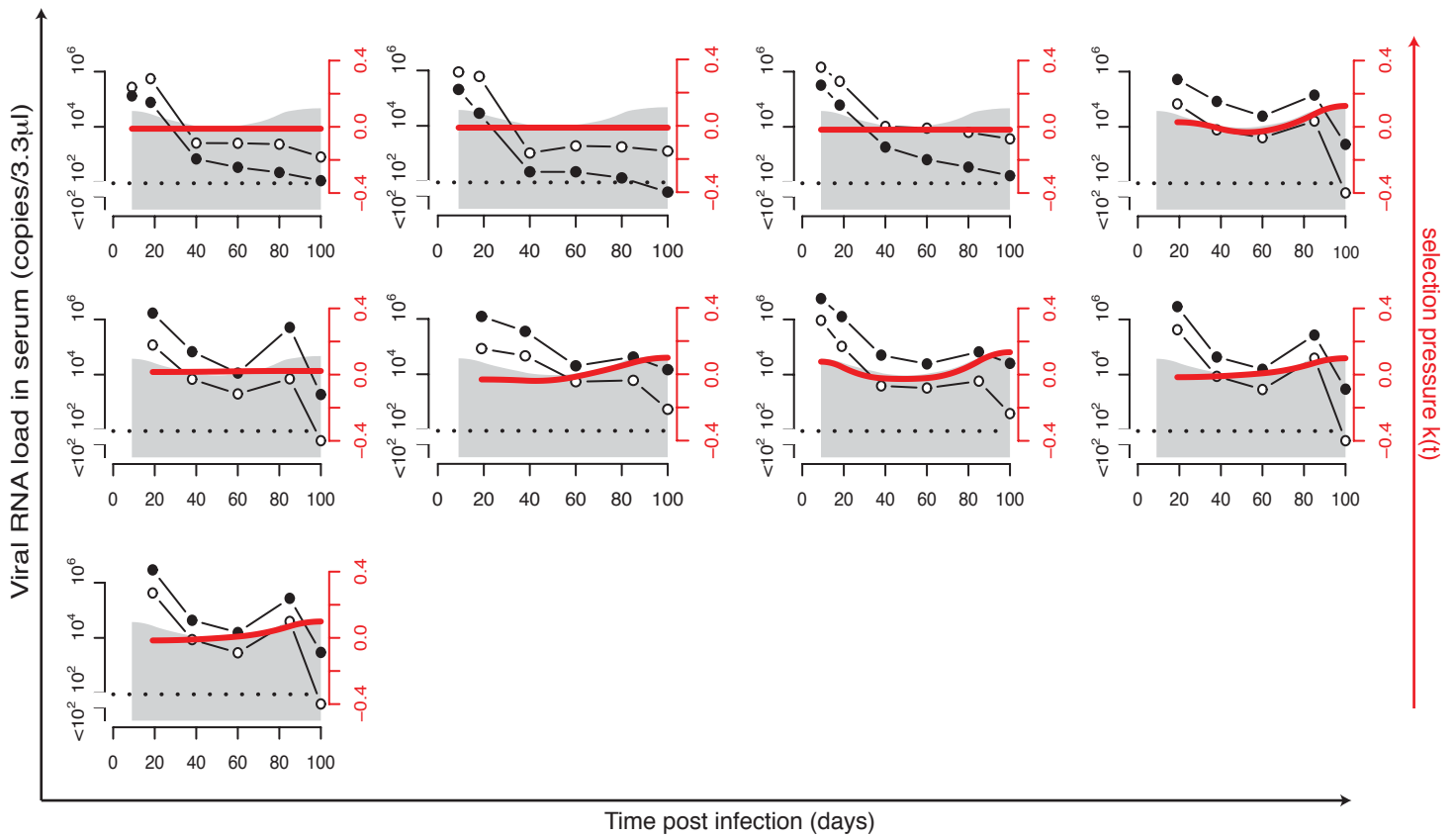
Figure S4

NP396

C57BL/6



BALB/c



● Epitope mutant virus ○ Wildtype virus █ 95% confidence interval — Selection pressure ..... qPCR detection limit



**Figure S4: NP396-specific CTL selection pressure in protracted LCMV infection.**

We infected C57BL/6 (top panels) and BALB/c mice (bottom panels) with  $2 \times 10^5$  PFU of  $\Delta$ NP396 virus in combination with  $2 \times 10^6$  PFU of wildtype LCMV (compare schematic in Fig. 1C). From serum samples collected on day 9, 20, 40, 60, 80 and 100 we quantified each virus individually by TaqMan RT-PCR (black circles :  $\Delta$ NP396; empty circles : wildtype virus). Time-dependent selection coefficients  $k(t)$  were calculated as schematically outlined in Figure 1G-I (for details see Materials & Methods) and are shown as red lines. The grey shaded area denotes the 95% confidence interval of background noise in  $k(t)$  in the absence of epitope-specific selection pressure. Each plot shows an individual C57BL/6 or BALB/c mouse from 2 experiments, which were combined for analysis. Select plots from this figure were chosen for display in Figure 2.